Journal of Applied Physics

Diamond nucleation in carbon films on Si wafer during microwave plasma enhanced chemical vapor deposition for quantum applications

Cite as: J. Appl. Phys. **133**, 155302 (2023); https://doi.org/10.1063/5.0143800
Submitted: 26 January 2023 • Accepted: 01 April 2023 • Published Online: 17 April 2023

Vidhya Sagar Jayaseelan and Raj N. Singh

AIP Publishing

Journal of Applied Physics ARTICLE scitation.org/journal/jap

Diamond nucleation in carbon films on Si wafer during microwave plasma enhanced chemical vapor deposition for quantum applications

Cite as: J. Appl. Phys. **133**, 155302 (2023); doi: 10.1063/5.0143800
Submitted: 26 January 2023 · Accepted: 1 April 2023 ·
Published Online: 17 April 2023

Vidhya Sagar Jayaseelan[a] and Raj N. Singh[b]

AFFILIATIONS

School of Materials Science and Engineering, Oklahoma State University, 700 N. Greenwood Avenue, HRC-200, Tulsa, Oklahoma 74016, USA

[a]**Current address:** Intel Corporation, 8695 NE Cornell Rd, Hillsboro, Oregon 97124, USA.
[b]**Author to whom correspondence should be addressed:** rajns@okstate.edu

ABSTRACT

Nucleation is important in processing of good quality diamond crystals and textured thin films by microwave plasma enhanced chemical vapor deposition (MPECVD) for applications in quantum devices and systems. Bias-enhanced nucleation (BEN) is one approach for diamond nucleation *in situ* during MPECVD. However, the mechanism of diamond nucleation by BEN is not well understood. This paper describes results on the nucleation of diamond within a carbon film upon application of electric field during the BEN-facilitated MPECVD process. The nature of the diamond film and nuclei formed is characterized by SEM (scanning electron microscopy), Raman spectroscopy, and high-resolution transmission electron microscopy (HRTEM). The HRTEM images and associated diffraction patterns of the nucleation layer show that the diamond nuclei are formed within the carbon film close to the Si (100) substrate surface under the influence of microwaves and electric fields that lead to formation of the textured diamond film and crystal upon further growth. These results are expected to develop diamond films of optimum quality containing a nitrogen-vacancy center for application in quantum systems.

INTRODUCTION

Diamond and other materials in the boron–carbon–nitrogen (B–C–N) ternary system are attractive because of their wide bandgap, optical transparency, and high thermal conductivity. These properties make diamond an ideal semiconductor for quantum electronics, optical devices, and thermal management of electronics for use in ambient as well as extreme conditions of high temperature and neutron irradiation.[1–5] In particular, diamond has point defects and defect centers with unusual properties for applications in quantum computing,[6] quantum entanglement,[7] encryption,[8] biolabeling,[9] and magnetic field sensing.[10] Nitrogen-vacancy (NV) centers in diamond have attracted significant attention for biological sensing,[11] quantum information processing,[12] and NMR (nuclear magnetic resonance) spectroscopy.[13] Qubit states (spins) of NV centers[14] can be controlled by microwave and optical signals, thereby rendering quantum network,[15] quantum memory,[16,17] and quantum sensing.[10] The NV centers in diamond are generally oriented randomly along four possible ⟨111⟩ directions. However, the need and challenge are to preferentially orient NV centers along one of the four ⟨111⟩ directions. The oriented NV centers are desirable for enhancing detectability using optically detected magnetic resonance (ODMR). We are addressing this challenge through our research based on appropriate selection of the substrate orientation and texturing of the grown diamond films *in situ* using bias-enhanced nucleation (BEN) followed by growth by microwave plasma enhanced chemical vapor deposition (MPECVD). A fundamental understanding of the diamond nucleation mechanism of BEN on Si substrates is also needed to achieve the goals of our research. To further explain our approach, we first describe how diamond is normally processed, which is followed by description of the important role of diamond nucleation and *in situ* doping to create NV defects in diamond.

Diamond powder for grinding and polishing is generally processed at high temperatures and high-pressures (HPHT) where it is thermodynamically stable and upon cooling retains the cubic phase

TABLE I. Process conditions used for the BEN and growth of diamond films.

Deposition parameters	Hydrogen etching	Carburization	Bias-enhanced nucleation	Growth
Duration of the step (min)	15	60	5 or 60	480
Bias voltage (V)	0	0	150	0
Substrate temperature (°C)	750	750	750	750
Pressure (Pa)	2666.4	2666.4	2666.4	12 670
H_2 flow (sccm)	100	100	100	39
CH_4 flow (sccm)	0	2	4	1
Ar flow (sccm)	0	0	0	60
Microwave power (W)	500	600	600	900

in ambient conditions. It can also be processed at low pressures in an activated plasma environment typical of a MPECVD. There are different approaches to processing diamond containing NV defects. These include detonation synthesis of diamond particles and HTHP for small diamond crystals.[18–20] MPECVD is the most promising approach for synthesizing diamond over a wider area on a variety of substrates, including on HPHT-synthesized single crystal diamond. MPECVD also offers much better control of diamond phase purity and crystalline defects as described in our research[2,21–29] and of many other researchers.[30–42]

The NV defect centers in diamond can be created *in situ* via doping with nitrogen (N) during MPECVD, which requires a fundamental understanding of the diamond nucleation and growth steps. Diamond does not nucleate homogeneously on most solid substrates because of the high surface energy. Thus, to process continuous diamond films on Si or other substrates by MPECVD, nucleation is encouraged by one of three ways, i.e., (1) seeding of the surface with nanodiamond particles, (2) ultrasonic agitation with diamond particles, and (3) scratching the surface. These approaches are used to facilitate heterogeneous nucleation sites followed by growth on already nucleated diamond. Narayan's group nucleated and grew diamond from carbon films by a novel approach of laser irradiation.[4,5] In addition, electrical bias-enhanced nucleation (BEN) in a plasma has been used for promoting nucleation *in situ* followed by growth to synthesize diamond thin films by MPECVD.[30–34] The BEN approach in combination with MPECVD also offers an independent control of the nitrogen doping via gaseous precursors of N_2 or NH_3 to grow diamond crystals and films for creating NV defect centers *in situ* of desired quality.

Bias-enhanced nucleation has been used by us and other researchers[30–34] for enhancing nucleation and promoting heteroepitaxial growth of diamond on Si and other substrates. In the BEN approach, a thin layer of carbon is deposited on the Si substrate followed by application of an electrical bias (100–300 V) *in situ* for a short duration (5–15 min), followed by growth, all in a MPECVD environment. Several mechanisms have been suggested for the nucleation process, such as super saturation of carbon at the surface,[34] enhanced surface mobility,[35] faster reaction rate at the surface,[36] formation of an epitaxial layer of SiC on Si,[37] and formation of a carbon layer that condenses to form epitaxial nuclei.[38] There is clearly no consensus among researchers on the mechanism of BEN. However, supporting evidence has been presented for each of these mechanisms although some contradict each other.

Therefore, the objectives of our research are to study and shed new insights on the fundamental of a diamond nucleation mechanism on an Si (100) substrate using BEN in a MPECVD process leading to formation of the textured diamond polycrystalline film. This paper describes results on the nucleation of diamond within the carbon film upon application of the bias electric field *in situ* during MPECVD. The nature of the diamond film and the nuclei formed are characterized by SEM, Raman spectroscopy, and HRTEM. The HRTEM images and associated diffraction patterns of the nucleation layer are used to show that diamond nuclei are formed within the carbon film close to the Si (100) substrate under the influence of microwave and electric fields that lead to a textured diamond film and oriented crystals within upon further growth. The textured diamond film is a promising host for promoting oriented NV centers *in situ* by MPECVD for a myriad of applications in quantum devices and systems.

EXPERIMENTAL METHODS

The deposition process was carried out in an ASTEX AX5100 MPECVD system, which has been described earlier in several of our publications.[21–29] To enable application of the electrical bias, a wire mesh screen made of a 0.3 mm diameter molybdenum wire was used that was held on a 2 mm diameter circular molybdenum wire. This wire mesh was inserted into the MPECVD chamber and held 20 mm above the substrate. The screen mesh was connected to one terminal of an MDX-500 DC power supply though an electrical feedthrough. The substrate holder and the MPECVD chamber were grounded as was the other terminal of the power supply.

P-type silicon (100) wafers diced into $2.54 \times 2.54\ cm^2$ squares were used as substrates. All substrates were etched in a standard hydrofluoric-nitric-acetic (HNA) acid solution (20 ml HF + 60 ml HNO_3 + 160 ml CH_3COOH) to remove any contaminated top layer. This was followed by cleaning the silicon pieces in a 2% HF solution in DI water to remove the native oxide layer before silicon pieces were placed inside the deposition chamber. The chamber was evacuated, and a base pressure of at least 1×10^{-5} Pa was achieved at a process temperature of 750 °C. The silicon was then etched in hydrogen plasma for 15 min at 2666.44 Pa, 100 sccm H_2 flow, and 500 W microwave power to remove surface impurities.

This was followed by a carburization step for 60 min in which 2 sccm of CH_4 was introduced into the chamber and the microwave power was increased to 600 W. Then, the bias voltage of +150 V was applied to the molybdenum screen mesh through the electrical feedthrough. The duration of the bias step was varied in the experiments. After the nucleation enhancement steps, the samples were placed in the deposition chamber and this time, the mesh was removed. Diamond films were grown on the pre-nucleated wafers in a 900 W plasma of H_2–Ar–CH_4 mixture at the ratio of 39:60:1 and at a pressure of 12 670 Pa. The substrate temperature as measured by a thermocouple below the substrate holder was around 750 °C. The growth step was carried out for 8 h followed by 15 min of hydrogen plasma etching to remove the carbon deposits. The growth conditions were selected based on the previous results that showed well-crystallized diamond grains with low secondary nucleation. A summary of the process conditions is given in Table I.

The samples were characterized by a Philips XL-30 FEG environmental scanning electron microscope (ESEM). Raman spectroscopy measurements were made using a model T 64000, Jobin Yvon triple monochromator system, equipped with an Olympus BX-41 microscope attachment. The Raman scattering was performed using a 514.5 nm Ar^+ ion laser. For the HRTEM study, free standing diamond thin films were prepared by etching the silicon substrate in an SF_6 rf-plasma etcher. The films were then ion milled either from both sides to study the bulk region of the film or exclusively from the top to characterize the nucleation layer. The HRTEM studies were performed using a Philips CM-20 transmission electron microscope (TEM).

RESULTS AND DISCUSSION

The SEM image from films grown after nucleation by the BEN technique is shown in Fig. 1. The samples nucleated for 5 min under a 150 V bias have led to formation of the oriented grains on the silicon substrate with the diamond [110] edges parallel to the Si [110] and the diamond (100) planes parallel to the Si (100) planes. Each of the grains has a pyramidal shape with a square base of (100) planes parallel to the Si (100) planes and four pyramidal planes (111) of a diamond crystal. This growth morphology of diamond crystals is consistent with the surface energies (γ) of different planes of diamond, i.e., $\gamma\ (111) < \gamma(110) < \gamma(100)$. A careful observation of individual grains also shows only slight misorientation between some of the grains in the x–y plane of the paper. On increasing the bias duration to 15 min, the fraction of grains that have identical x–y orientation is reduced quite drastically (not included in this paper), which confirmed that there is an optimum bias duration for nucleation and growth of the oriented and textured diamond crystals. This observation then prompted us to explore the nature of the diamond nucleation process in more detail using HRTEM that led to the oriented/textured growth of diamond thin films shown in Fig. 1.

The thin sections of the diamond film suitable for an HRTEM study were prepared by a combination of rf plasma etching using SF_6 and ion milling using Ar as described earlier. These approaches led to thin foils near the Si–diamond interface from the nucleating region. The HRTEM images of the nucleation layer of the diamond film created by 5 min of BEN at 150 V are shown in Fig. 2. Figure 2 shows that the majority of the area is covered by small almost circular/spherical nuclei of the order of about 5–10 nm diameter.

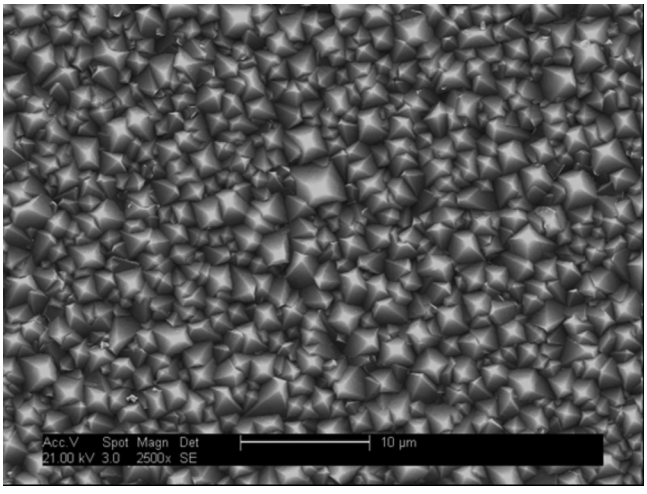

FIG. 1. SEM of oriented and textured diamond films nucleated by BEN at 150 V for 5 min and grown using MPECVD on an Si (100) substrate. The majority of diamond crystals are oriented similarly in the x–y plane leading to high degree of pyramidal shape and texture.

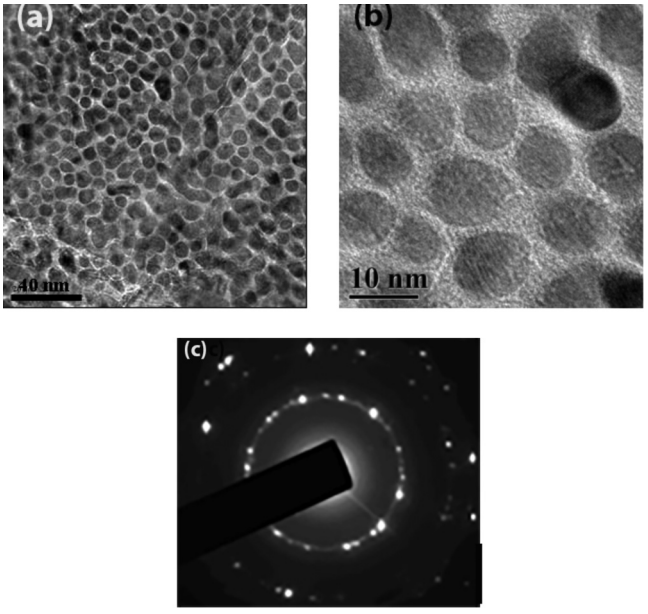

FIG. 2. HRTEM images [(a) and (b)] from a nucleating layer of diamond on an Si (100) substrate upon BEN for 5 min at 150 V showing nucleation of diamond nano-grains in an amorphous carbon created during carburization treatment. Some of these nano-diamond nuclei show lattice fringes indicating diamond crystal formation. Also shown is an electron diffraction pattern (c) from the nucleating layer consistent with the diamond crystal lattice.

These nanometer size nuclei are separated by an intermediate region of about 2–3 nm. The darker nuclei in the higher magnification image in Fig. 2(b) show parallel lattice patterns, indicating nucleation of the crystalline diamond. The electron diffraction pattern from this region of the nucleating layer is shown in Fig. 2(c). It has bright spots located on circular rings at a distance/reciprocal space typically seen for a well-crystallized diamond film or crystal. The first ring is from a diamond plane (111), the second from a plane (220), and the third from a plane (311). There is also a large and bright diffused spot at the center of the diffraction pattern, which can be attributed to an amorphous phase of carbon created during carburization and BEN steps during processing by MPECVD. These observations suggest that diamond nuclei are formed and crystallized in the amorphous carbon film created as a result of the carburization, BEN, and exposure to microwave plasma. The crystallization of an amorphous carbon film to isolated diamond nuclei appears to be caused by bias and microwave plasma during processing, which seem to be the most likely explanation for the circular/spherical morphology of nuclei observed in Fig. 2. The small size of the nuclei near the Si substrate ensures their strong interaction with the substrate leading to preferred orientation of diamond upon further growth. It is well-known that processing of a diamond film by MPECVD involves deposition of both sp^3 and sp^2 carbons. However, there is also plasma etching underway simultaneously in the plasma environment, which etches away a softer sp^2 carbon leaving behind an essentially phase pure diamond phase with an sp^3-bonded carbon. This hypothesis is further explored through Raman analyses of films obtained from different stages of processing, including BEN and plasma etching as described next.

In this approach, the deposited film was removed after BEN steps and characterized using Raman spectroscopy. Then, this film was plasma-etched to remove a non-diamond carbon phase preferentially and characterized again by Raman spectroscopy. The plasma etching was done by exposing the film to a plasma in the same MPECVD reactor under the conditions of a microwave power of 900 W, a pressure of 12 670 Pa, and gas flow rates of 60 sccm Ar and 40 sccm H_2. The plasma etching was done for 120 min. Since no carbon precursor is present in the plasma etching gases, there is no possibility of diamond or carbon formation during etching. This plasma etching procedure is expected to reveal the relative effects of the plasma on the components of the previously formed BEN layer. The Raman spectra of films before and after plasma etching are shown in Fig. 3(a). Also, included are Raman spectra from a single crystal diamond (HPHT-synthesized) and a sample of CVD graphite. A strong first order phonon peak at 1333 cm^{-1} is from single crystal diamond. The CVD graphite shows strong peaks at 1352 cm^{-1}, 1585 cm^{-1}, and a shoulder at 1615 cm^{-1} associated with D, G bands of graphite, and disordered or amorphous carbon, respectively. The Raman spectrum for the BEN film deposited for 1 h [1 h BEN shown in Fig. 3(a)] looks more like CVD graphite except that both peaks are broadened in comparison with the CVD graphite, and the D band of graphite is clearly shifted toward the peak at 1332 cm^{-1}, which is attributed to diamond. These observations suggest that deposition of a film under BEN and in an MPECVD environment forms carbon containing both sp^2- and sp^3-bonded carbons. This film was then Ar–H_2 plasma-etched in the MPECVD system for 2 h, and the Raman spectrum from an etched film shows a strong peak at 1332 cm^{-1} and very weak peaks at ~1455 and ~1550 cm^{-1}. These observations indicated that the plasma etching basically removes the non-diamond sp^2 carbon leaving behind an sp^3-bonded carbon from the diamond phase.

The Raman spectra obtained from the BEN film before and after plasma etching were analyzed using PeakFit software.[39] In this approach, the experimentally observed spectrum is deconvoluted into different Raman peaks originating from different phases of carbon and diamond. Then, these peaks are used in the software to determine the fitted spectrum by adjusting the peak height, width, and position parameters. The analysis of this type of data can give quantitative estimates of the different phases forming the film after due correction from the Raman scattering cross sections of different phases. The Raman spectra in the range of 1000–1700 cm^{-1} were baseline corrected, smoothened for noise, and fit with the Lorentzian function for the diamond peaks and the Gaussian function for the non-diamond components. The results are presented in Figs. 3(b) and 3(c). Figures 3(b) shows results for the as-deposited 1-h BEN film fitted using four Raman peaks located at 1209, 1335, 1505, and 1585 cm^{-1}. The peak at 1209 is attributed to *trans*-polyacetylene segments at grain boundaries and surfaces. The peak at 1335 is attributed to the first order phonon peak of diamond broadened by phonon confinement. The peak at 1505 is attributed to the I-band from amorphous carbon or sp2 carbon clusters. The peak at 1585 is attributed to the G band of graphite-like inclusions or amorphous carbon. Therefore, the Raman spectra in Fig. 3(b) suggest nucleation of an sp^3 carbon in a matrix of an sp^2 carbon because of the BEN.

Figure 3(c) shows results for the plasma-etched film fitted using seven different peaks located at 1175 (attributed to *trans*-polyacetylene), 1284 (attributed to a disordered carbon phase), 1330 (attributed to a first order phonon peak of diamond), 1371 (attributed to a D-peak associated with a disordered carbon), 1445 (attributed to amorphous polyacetylene bonds), 1543 (attributed to a G-band of graphite-like inclusions or an amorphous carbon), and 1607 (attributed to an amorphous carbon or microcrystalline graphite). The appearance of the diamond first order Raman line in the etched BEN film at 1332 cm^{-1} is clearly evident. In addition, a strong reduction in the amplitude of the G band from an sp^2 carbon peak at 1580 cm^{-1} is also observed in the etched film when compared with the BEN film, indicating a reduction in the sp^2 and amorphous carbon content in the etched film. A dominant broad peak at around 1450 cm^{-1} associated with the I-band of the carbon is found in the etched film. Though this peak is frequently associated with an amorphous carbon or sp^2 carbon clusters of various sizes, it is commonly seen in low quality as grown CVD diamond films. These results indicate that the amorphous carbon formed under the carburization and BEN steps are etched away by the Ar-H_2 plasma. Furthermore, observations from Raman analyses of samples obtained from different stages of processing suggest that diamond nuclei shown in Figs. 2(a) and 2(b) are formed in the amorphous carbon phase in the proximity of the Si-substrate because of the biasing electric field and microwave plasma environments. These nuclei then act as a seed for further growth and coalescence leading to textured and faceted polycrystalline diamond film processed in the MPECVD as shown in Fig. 1.

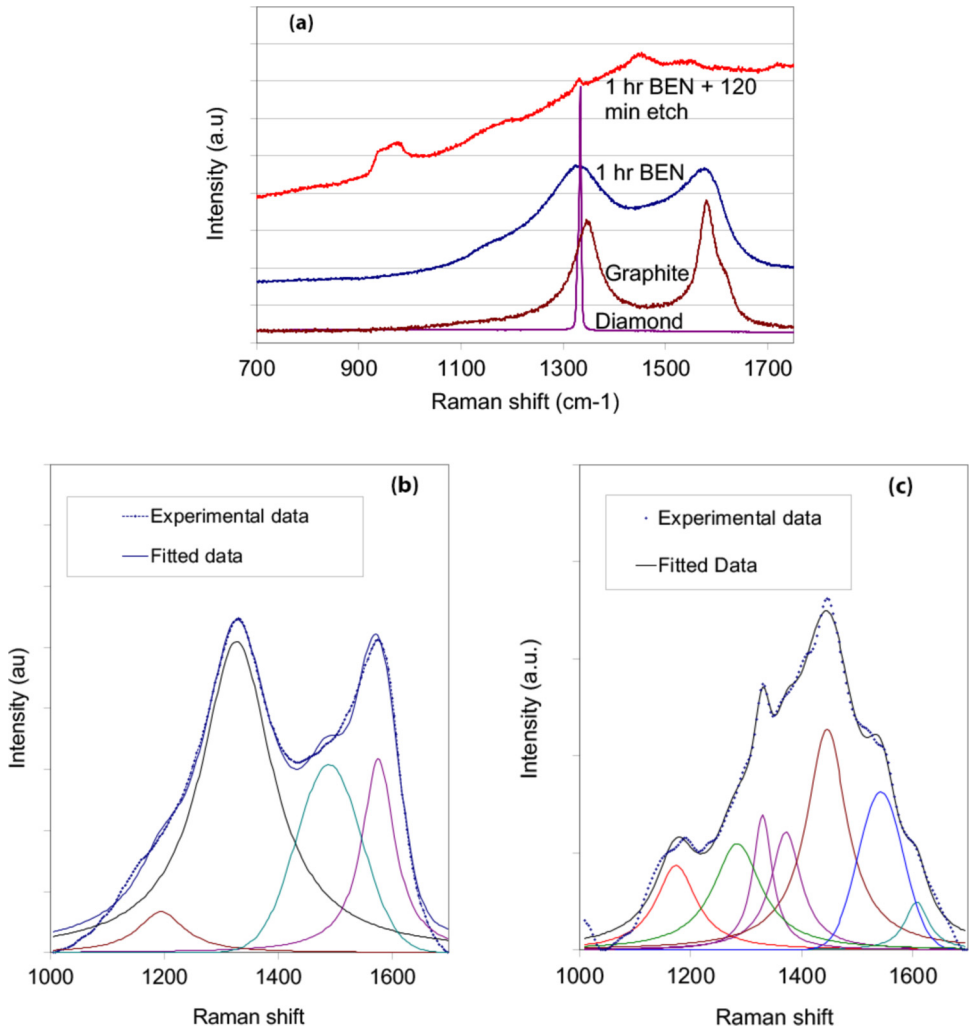

FIG. 3. Raman spectra from (a) a diamond film deposited for 1 h under a 150 V bias followed by H_2–Ar plasma etching for 120 min. Also shown are Raman spectra from a single crystal diamond (HPHT-synthesized) and a sample of CVD graphite. Fitting of the experimental Raman spectrum after smoothening and baseline subtraction with the Lorentzian function for the diamond peaks and Gaussian for the non-diamond components for (b) the 60 min BEN film and (c) the 60 min BEN film followed by 120 min plasma etching. The deconvoluted peaks are also shown.

Some researchers[37] have suggested that formation of SiC nuclei on an Si substrate during BEN is responsible for diamond nucleation. However, neither the HRTEM results from the nucleation layer nor the Raman data provided any evidence of SiC formation. The strong Raman peaks for a 6H-SiC polytype are generally observed at 505, 768, 796, 888, and 966 cm^{-1}.[40] For the cubic 3C-SiC polytype, the strong Raman peaks are at 795 and 973 cm^{-1}.[40] We did not find any evidence of SiC-related Raman peaks in the BEN films, which indicated that SiC formation cannot be attributed to diamond nucleation during BEN and MPECVD of diamond films.

The findings from this research are important for processing diamond containing nitrogen-vacancy centers (NV) for quantum devices. Most researchers have used HPHT-synthesized tiny diamond crystals and grown diamond films on diamond crystals. Then, they implant nitrogen and anneal at high temperatures (1200–1500 °C) to create NV centers. This complicates processing of devices and limits widespread applications to quantum devices and systems. In this research, we have shown that textured polycrystalline diamond films of good quality can be processed through understanding of the nucleation mechanism of BEN. In the future, we plan to explore *in situ* doping of nitrogen during growth by MPECVD. In addition, the texture of diamond crystals grown in the Z-direction and the XY plane can be controlled using some of our approaches, which are expected to offer many more possibilities for achieving preferred orientation of the NV centers in diamond for applications in quantum systems. We had previously done research on diamond doping *in situ* by nitrogen and pursuing it at the present for creating NV centers. The optimum nitrogen doping level has to be determined, but it should not be too high for preserving a diamond crystal structure. The quality of NV centers, thus, created will be characterized by ODMR (optically detected magnetic resonance) and PL techniques, which will provide feedback on the processing of optimum quality NV centers in diamond films by MPECVD.

CONCLUSIONS

The diamond nucleation mechanism responsible for creating textured diamond films on Si wafers using BEN and MPECVD was studied. SEM results from the grown diamond film on an Si (100) substrate indicated that highly textured films with diamond grains displaying pyramidal morphology and preferred orientation within the x–y plane of most diamond crystals were processed. HRTEM images from the nucleating layer on an Si (100) substrate showed formation of circular/spherical diamond nuclei of ∼5–10 nm diameter within the amorphous or sp^2 carbon film that formed during the BEN and MPECVD process. Raman spectroscopy data of the carbon film formed during BEN and MPECVD further indicated that the diamond nucleated and crystallized within the carbon film. The diamond nuclei then grew further upon MPECVD in which the sp^2 carbon etched away by the plasma leading to formation of diamond films with excellent texture within the x–y plane and along the z direction. HRTEM and Raman data from the nucleating layer did not show any evidence of an SiC phase, which suggested that the diamond nucleation is not related to SiC formation on the Si substrate.

These results provided a fundamental understanding of diamond nucleation for processing diamond films and crystals of improved quality for a myriad of quantum devices and applications.

ACKNOWLEDGMENTS

This material was based on the work supported by the National Science Foundation under NSF Award Nos. 2103058 and 2126275. Any opinions, findings, and conclusions or recommendations expressed in this material are those of the authors and do not reflect views of the National Science Foundation.

AUTHOR DECLARATIONS

Conflict of Interest

The authors have no conflicts to disclose.

Author Contributions

Vidhya Sagar Jayaseelan: Conceptualization (equal); Data curation (equal); Formal analysis (equal); Funding acquisition (equal); Investigation (equal); Methodology (equal); Project administration (equal); Resources (equal); Supervision (equal); Validation (equal); Writing – original draft (equal). **Raj N Singh:** Conceptualization (equal); Data curation (equal); Formal analysis (equal); Funding acquisition (equal); Investigation (equal); Methodology (equal); Project administration (equal); Resources (equal); Supervision (equal); Validation (equal); Writing – original draft (equal).

DATA AVAILABILITY

The data that support the findings of this study are available within the article.

REFERENCES

[1]D. Das and R. N. Singh, "A review on nucleation, growth, and low-temperature synthesis of diamond thin films," Int. Mater. Rev. **52**(1), 29–64 (2007).
[2]C. B. Samantaray and R. N. Singh, "A review of synthesis and properties of cubic boron nitride thin films," Int. Mater. Rev. **50**(6), 313–344 (2005).
[3]M. Jana and R. N. Singh, "A review: Progress in CVD synthesis of layered hexagonal boron nitride with tunable properties and their applications," Int. Mater. Rev. **63**, 162 (2018).
[4]J. Narayan and A. Bhaumik, "Novel phase of carbon, ferromagnetism, and conversion into diamond," J. Appl. Phys. **118**, 215303 (2015).
[5]A. Bhaumik, R. Sachan, and J. Narayan, "Tunable charge states of nitrogen-vacancy centers in diamond for ultrafast quantum devices," Carbon **142**, 662–672 (2019).
[6]J. Wrachtrup and F. Jelezko, "Processing quantum information in diamond," J. Phys.: Condens. Matter **18**(21), S807–S824 (2006).
[7]B. Hensen, H. Bernien, A. E. Dréau, A. Reiserer, N. Kalb, M. S. Blok, J. Ruitenberg, R. F. L. Vermeulen, R. N. Schouten, C. Abellán, W. Amaya, V. Pruneri, M. W. Mitchell, M. Markham, D. J. Twitchen, D. Elkouss, S. Wehner, T. H. Taminiau, and R. Hanson, "Experimental loophole-free violation of a Bell inequality using entangled electron spins separated by 1.3 km," Nature **526**(7575), 682–686 (2015).
[8]M. Hirose and P. Cappellaro, "Coherent feedback control of a single qubit in diamond," Nature **532**(7597), 77–80 (2016).
[9]B. M. Chang, H. H. Lin, L. J. Su, W.-D. Lin, R. J. Lin, Y. K. Tzeng, R. T. Lee, Y. C. Lee, A. L. Yu, and H. C. Chang, "Highly fluorescent nanodiamonds protein-functionalized for cell labeling and targeting," Adv. Funct. Mater. **23**(46), 5737–5745 (2013).
[10]J. R. Maze, P. L. Stanwix, J. S. Hodges, S. Hong, J. M. Taylor, P. Cappellaro, L. Jiang, M. V. G. Dutt, E. Togan, A. S. Zibrov, A. Yacoby, R. L. Walsworth, and M. D. Lukin, "Nanoscale magnetic sensing with an individual electronic spin in diamond," Nature **455**(7213), 644–647 (2008).
[11]A. Gruber, A. Dräbenstedt, C. Tietz, L. Fleury, J. Wrachtrup, and C. V. Borczyskowski, "Scanning confocal optical microscopy and magnetic resonance on single defect centers," Science **276**(5321), 2012–2014 (1997).
[12]E. Neu, D. Steinmetz, J. Riedrich-Möller, S. Gsell, M. Fischer, M. Schreck, and C. Becher, "Single photon emission from silicon-vacancy colour centres in chemical vapour deposition nano-diamonds on iridium," New J. Phys. **13**, 025012 (2011).
[13]I. Lovchinsky, A. O. Sushkov, E. Urbach, N. P. de Leon, S. Choi, K. De Greve, R. Evans, R. Gertner, E. Bersin, C. Müller, L. McGuinness, F. Jelezko, R. L. Walsworth, H. Park, and M. D. Lukin, "Nuclear magnetic resonance detection and spectroscopy of single proteins using quantum logic," Science **351**(6275), 836–841 (2016).
[14]C. G. Yale, B. B. Buckley, D. J. Christle, G. Burkard, F. J. Heremans, L. C. Bassett, and D. D. Awschalom, "All-optical control of a solid-state spin using coherent dark states," Proc. Natl. Acad. Sci. U.S.A. **110**(19), 7595–7600 (2013).
[15]H. Bernien, B. Hensen, W. Pfaff, G. Koolstra, M. S. Blok, L. Robledo, T. H. Taminiau, M. Markham, D. J. Twitchen, L. Childress, and R. Hanson, "Heralded entanglement between solid state qubits separated by three meters," Nature **497**(7447), 86–90 (2013).
[16]P. C. Maurer, G. Kucsko, C. Latta, L. Jiang, N. Y. Yao, S. D. Bennett, F. Pastawski, D. Hunger, N. Chisholm, M. Markham, D. J. Twitchen, J. I. Cirac, and M. D. Lukin, "Room-temperature quantum bit memory exceeding one second," Science **336**(6086), 1283–1286 (2012).
[17]A. Haque and S. Sumaiya, "An overview on the formation and processing of nitrogen-vacancy photonic centers in diamond by ion implantation," J. Manuf. Mater. Process. **1**(1), 1–16 (2017).
[18]V. N. Mochalin, O. Shenderova, D. Ho, and Y. Gogotsi, "The properties and applications of nanodiamonds," Nat. Nanotechnol. **7**(1), 11–23 (2012).
[19]J.-P. Boudou, P. A. Curmi, F. Jelezko, J. Wrachtrup, P. Aubert, M. Sennour, G. Balasubramanian, R. Reuter, A. Thorel, and E. Gaffet, "High yield fabrication of fluorescent nanodiamonds," Nanotechnology **20**(23), 235602 (2009).
[20]Y. Chu, N. de Leon, B. Shields, B. J. M. Hausmann, R. Evans, M. J. Burek, M. Markham, A. Stacey, A. Zibrov, D. Twitchen, M. Loncar, H. Park, P. Maletinsky, and M. D. Lukin, "Coherent optical transitions in implanted nitrogen vacancy centers," Nano Lett. **14**, 1982–1986 (2014).

[21]N. Govindaraju and R. N. Singh, "Effect of microwave plasma process conditions on nanocrystalline diamond deposition on AlGaN/GaN HEMT and Si device metallizations," Ceram. Trans. **234**, 99–113 (2012).
[22]N. Govindaraju, D. Das, R. N. Singh, and P. B. Kosel, "Comparison of the electrical behavior of AlN-on-diamond and AlN-on-Si MIS rectifying structures," Ceram. Trans. **235**, 77–86 (2012).
[23]N. Govindaraju, P. B. Kosel, and R. N. Singh, "Effect of nanocrystalline diamond deposition conditions on Si MOSFET device characteristics," Ceram. Trans. **235**, 87–93 (2012).
[24]N. Govindaraju and R. N. Singh, "Processing of nanocrystalline diamond thin films for thermal management of wide bandgap semiconductor power electronics," Mater. Sci. Eng. B **176**(14), 1058–1072 (2011).
[25]N. Govindaraju, C. Kane, and R. N. Singh, "Processing of multilayered nanocrystalline and microcrystalline diamond thin films using Ar-rich microwave plasmas," J. Mater. Res. **26**(24), 3072–3082 (2011).
[26]N. Govindaraju, D. Das, P. B. Kosel, and R. N. Singh, "High-temperature dielectric behavior of nanocrystalline and microcrystalline diamond thin films," ECS Trans. **33**(13), 155–168 (2010).
[27]N. Govindaraju, D. Das, R. N. Singh, and P. B. Kosel, "High-temperature electrical behavior of nanocrystalline and microcrystalline diamond films," J. Mater. Res. **23**(10), 2774–2786 (2008).
[28]D. Das, R. N. Singh, S. Chattopadhyay, and K. H. Chen, "Thermal conductivity of diamond films deposited at low surface temperatures," J. Mater. Res. **21**(9), 2379–2388 (2006).
[29]D. Das, V. Jayaseelan, R. Ramamurti, R. S. Kukreja, L. Guo, and R. N. Singh, "Low surface temperature synthesis and characterization of diamond thin films," Diamond Relat. Mater. **15**, 1336–1349 (2006).
[30]B. R. Stoner, G.-H. M. Ma, S. D. Wolter, and J. T. Glass, "Characterization of bias-enhanced nucleation of diamond on silicon by *in vacuo* surface analysis and transmission electron microscopy," Phys. Rev. B **45**(19), 11067–11084 (1992).
[31]A. Saravanan, B.-R. Huang, K. J. Sankaran, S. Kunuku, C.-L. Dong, K.-C. Leou, N.-H. Tai, and I.-N. Lin, "Bias-enhanced nucleation and growth processes for ultrananocrystalline diamond films in Ar/CH4 plasma and their enhanced plasma illumination properties," ACS Appl. Mater. Interfaces **6**, 10566–10575 (2014).
[32]K. Janischowsky, W. Ebert, and E. Kohn, "Bias enhanced nucleation of diamond on silicon (100) in a HFCVD system," Diamond Relat. Mater. **12**, 336–339 (2003).
[33]W. Kulisch, L. Ackerman, and B. Sobisch, "On the mechanisms of bias enhanced nucleation of diamond," Phys. Status Solidi A **154**, 155–174 (1996).
[34]S. Yugo, T. Kanai, T. Kimura, and T. Muto, "Generation of diamond nuclei by electric field in plasma chemical vapor deposition," Appl. Phys. Lett. **58**(1011), 1036–1038 (1991).
[35]N. Ishigaki and S. Yugo, "Mechanism of diamond epitaxial growth on silicon," Diamond Relat. Mater. **9**, 1646–1649 (2000).
[36]X. Jiang, K. Schiffmann, A. Westphal, and C. P. Klages, "Atomic-force-microscopic study of heteroepitaxial diamond nucleation on (100) silicon," Appl. Phys. Lett. **63**(9), 1203–1205 (1993).
[37]Y. K. Kim, K. H. Lee, M. J. Lee, and J. Y. Lee, "The nucleation of highly oriented diamond on silicon using a negative bias," Thin Solid Films **341**, 211–215 (1999).
[38]B. Golding, C. Bednarski-Meinke, and Z. Dai, "Diamond heteroepitaxy: Pattern formation and mechanisms," Diamond Relat. Mater. **13**, 545–551 (2004).
[39]Peakfit 4.0 for Windows, User's Manual, Peak Separation and Analysis software, AISN Software, SPSS Inc., Chicago, IL, 1997.
[40]G. Chikvaidze, N. Mironova-Ulmane, A. Plaude, and O. Sergeev, "Investigation of silicon carbide polytypes by Raman spectroscopy," Latv. J. Phys. Tech. Sci. **51**, 51–57 (2014).
[41]S. Mandal, "Nucleation of diamond films on heterogeneous substrates: A review," RSC Adv. **11**, 10159 (2021).
[42]S. A. Linnik, A. V. Gaydaychuk, A. S. Mitulinsky, and S. P. Zenkin, "Radio frequency bias enhanced nucleation of CVD diamond," Mater. Lett. **324**, 132670 (2022).